CHEMISTRY OF MATERIALS

ARTICLE

pubs.acs.org/cm

Dicyanovinylene-Substituted Selenophene−Thiophene Co-oligomers for Small-Molecule Organic Solar Cells

Stefan Haid,[†] Amaresh Mishra,*[,†] Christian Uhrich,[‡] Martin Pfeiffer,[‡] and Peter Bäuerle*[,†]

[†]Institute of Organic Chemistry II and Advanced Materials, University of Ulm, Albert-Einstein-Allee 11, D-89081 Ulm, Germany

[‡]Heliatek GmbH, Treidlerstrasse 3, 01139 Dresden, Germany

Supporting Information

ABSTRACT: We report on the design, synthesis, and characterization of a series of terminal dicyanovinylene-substituted quinquechalcogenophenes as light-harvesting small-molecule donor materials for organic solar cells. The spectroscopic, electrochemical, and thermal properties of these pentamers were investigated. The replacement of thiophene unit(s) by selenophene(s) results in a bathochromic shift of the longest wavelength absorption band with concomitant increase of the molar extinction coefficient. Cyclic voltammetry measurements revealed fully reversible oxidation and irreversible reduction processes. The highest occupied and lowest unoccupied molecular orbital (HOMO/LUMO) energy levels were determined from electrochemical measurements and lie in the range of −5.6 and −3.8 eV. Vacuum-deposited bulk-heterojunction solar cells fabricated with the novel chalcogenophenes as donor and C_{60} as acceptor displayed high open-circuit voltages of up to 1 V, short-circuit currents close to 8 mA·cm^{-2}, and power conversion efficiencies over 3%.

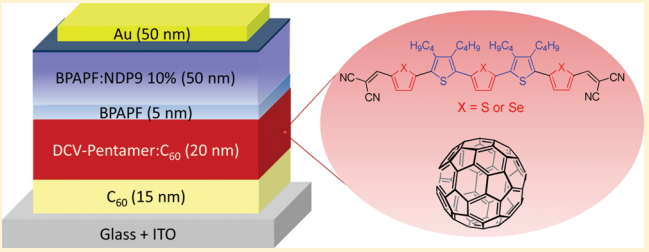

KEYWORDS: oligothiophene, selenophene, dicyanovinylene acceptor, bulk-heterojunction solar cells, structure−property relationship

INTRODUCTION

In the past decade, organic solar cells (OSC) have been intensely investigated because very thin devices can be fabricated on flexible substrates with low material consumption.[1−4] In the fields of both small-molecule and polymer solar cells, an enormous increase in power conversion efficiencies has been achieved in recent years, from under 1% in the beginning to currently over 7%.[5−13] Very recently, certified power conversion efficiencies of 8.3% have been independently released for a tandem cell prepared by the combination of two BHJ devices based on small molecules by Heliatek GmbH and for solution-processed polymer solar cells by Konarka.[14] Small molecules offer several advantages compared to their polymeric counterparts, such as well-defined structure, efficient functionalization, and purification. Most importantly in the case of small molecules, batch variations, which can affect polymers, can be avoided.

Small-molecule organic solar cells (SMOSC) can be prepared either from solution or by vacuum processing. In the latter case, very good efficiencies were achieved by use of various small molecules as light-harvesting electron-donor materials and C_{60} as acceptor.[12,15−23] Especially, dicyanovinylene (DCV) -substituted oligothiophenes showed very promising photovoltaic properties. In a series of DCV-substituted oligothiophenes with butyl side chains in the β-positions of the oligothiophene backbone, the quinquethiophene (DCV5T) showed the best performance with a high open-circuit voltage (V_{OC}) of 1.0 V and an efficiency of 3.4% in planar heterojunction (PHJ) solar cells.[15,16] The high V_{OC} obtained in these cells can be ascribed to the relatively deep-lying highest occupied molecular orbital (HOMO) energy level at −5.6 eV versus vacuum. It is well-established that the V_{OC} is related to the difference between the HOMO energy level of the donor and the lowest unoccupied molecular orbital (LUMO) energy level of the acceptor.[24,25] Replacement of the butyl chains by ethyl chains resulted in a decrease in efficiency (2.5%) due to a lower fill factor (FF).[26] Vacuum processing also allows the fabrication of bulk-heterojunction (BHJ) solar cells by coevaporation of donor and acceptor components. Very recently, by use of a nonalkylated DCV-substituted quinquethiophene as donor in p-i-n-type BHJ devices, record efficiencies of 5.2% were achieved.[12] The BHJ layer was prepared by coevaporation of the quinquethiophene donor and the C_{60} acceptor. With this BHJ structure, the donor−acceptor interface area is highly increased, thus ensuring more efficient charge separation. Furthermore, the resulting interpenetrating network facilitates charge transport.

While oligo- and polythiophenes are among the best investigated materials in the field of organic electronics,[6,27] oligo- and polyselenophenes were only scarcely investigated. Nevertheless, they show some promising properties, especially for application

Received: May 17, 2011
Revised: September 1, 2011
Published: September 26, 2011

in organic solar cells, that is, lower band gaps, red-shifted absorption, good polarizability, and improved interchain charge transfer.[28−33] Despite these favorable properties, only very few polyselenophenes and selenophene-containing copolymers were tested in polymer solar cells; they showed efficiencies in the range 0.1−2.7%.[34−37] There are as well only a few examples for selenophene-based sensitizers in dye-sensitized solar cells (DSSC).[38,39] Until now, there has been only one example of a SMOSC using a selenophene-containing donor material.[40] In that report, solution-processed BHJ solar cells were fabricated from selenophene-substituted diketopyrrolopyrrole derivatives, giving efficiencies of 1.5%.

In this study, we present the synthesis of three DCV-end-capped quinquechalcogenophenes with increasing number of selenophene units from one to three (Figure 1). The mixed oligomers are compared to parent oligothiophene DCV5T, which lacks selenophene units. The effects of increasing selenophene content on optical, electrochemical, and thermal properties are investigated, and good structure−property relationships were deduced. Furthermore, the fabrication of vacuum-processed BHJ solar cells with these compounds is described, leading to very promising results.

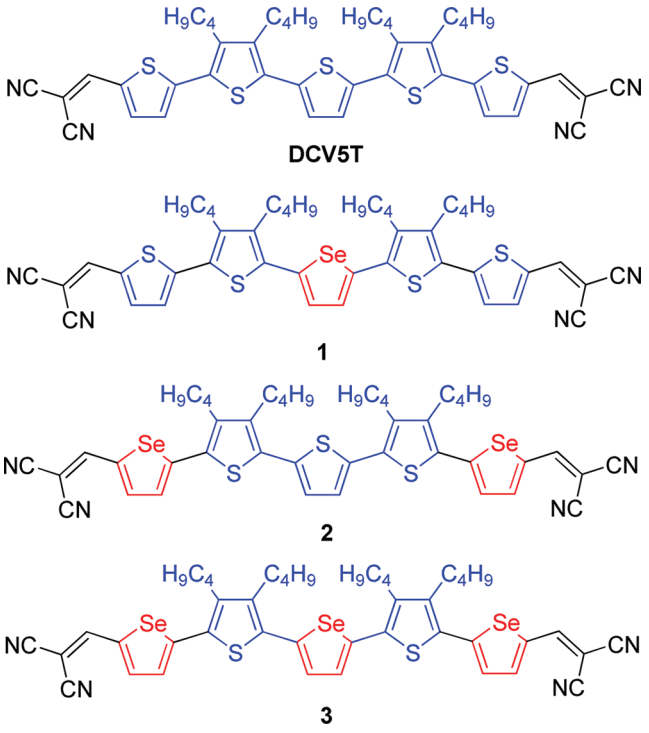

Figure 1. Investigated chalcogenophenes.

RESULTS AND DISCUSSION

Synthesis. Synthesis of parent **DCV5T** is described in the literature.[15] Co-oligomers **1**−**3** were synthesized in a similar fashion via palladium-catalyzed cross-coupling reactions. The synthesis of **1** and **3** (Scheme 1) started with selenophene **4**, which was dibrominated with *N*-bromosuccinimide (NBS) to afford 2,5-dibromoselenophene **5** in 84% yield. The latter compound was coupled with dibutylated thiophene boronic ester **7** in a Suzuki-type cross-coupling reaction to obtain dithienylselenophene **8** in 82% yield.

Mixed trimer **8** was diiodinated with iodine/mercury(II) acetate in chloroform to give diiodinated trimer **9** in a yield of 95%. Pentamer **12a** was prepared in 93% yield by a Stille-type coupling reaction of **9** and tributylstannyl thiophene **10** in dimethylformamide (DMF) at 75 °C. On the other hand, Pd^0-catalyzed Suzuki cross-coupling reaction of **9** with selenophene boronic ester **11** gave **12b** in 96% yield. Mixed pentamers **12a** and **12b** were then further functionalized in a Vilsmeier−Haack

Scheme 1. Synthesis of Pentamers 1 and 3[a]

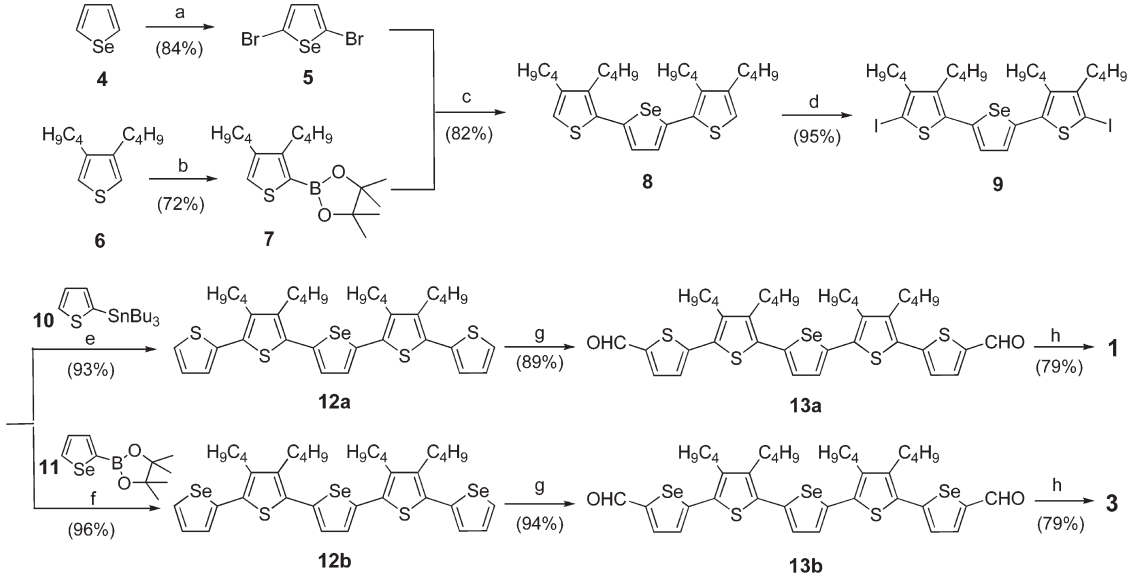

[a] (a) NBS (2 equiv), DMF, room temperature (rt), 16 h. (b) (i) *n*-BuLi, THF, 0 °C; (ii) 2-isopropoxy-4,4,5,5-tetramethyl-1,3,2-dioxaborolane. (c) $Pd_2(dba)_3$, $HP^tBu_3BF_4$, aq K_3PO_4, THF, 50 °C, overnight. (d) I_2/$Hg(OAc)_2$, $CHCl_3$, 0 °C to rt. (e) 2-Tributylstannylthiophene **10**, $Pd(PPh_3)_2Cl_2$, THF, 75 °C, 3 days. (f) 4,4,5,5-Tetramethyl-2-(selenophen-2-yl)-1,3,2-dioxaborolane **11**, $Pd_2(dba)_3$, $HP^tBu_3BF_4$, aq K_3PO_4, THF, rt, overnight. (g) $POCl_3$/DMF, DCE, rt, 22 h. (h) Malononitrile, β-alanine, DCE/EtOH, reflux, 24 h.

dx.doi.org/10.1021/cm201392c |*Chem. Mater.* 2011, 23, 4435–4444

formylation with $POCl_3$/DMF in dichloroethane to afford dialdehydes **13a** and **13b** in 89% and 94% yield, respectively. In a final step, the dialdehydes were transformed into the corresponding dicyanovinylene compounds by Knoevenagel condensation with malononitrile and β-alanine in a dichloromethane/ethanol mixture. Thus, co-oligomers **1** and **3** were obtained in 79% yield each.

Synthesis of co-oligomer **2** started from 5-bromoselenophene-2-carbaldehyde **14** and tetrabutylated terthiophene **16** (Scheme 2). Aldehyde **14**[41] was condensed with malononitrile in a Knoevenagel condensation to afford brominated DCV-substituted selenophene **15** in 84% yield. Terthiophene **16**[42] was distannylated by lithiation using *n*-butyllithium in the presence of tetramethylethylenediamine (TMEDA) and subsequently quenched with trimethyltin chloride. Distannylated terthiophene **17** was obtained in 83% yield. Final Pd^0-catalyzed Stille-type cross-coupling of **15** and **17** in DMF at 75 °C afforded mixed pentamer **2** in 67% yield. All DCV-substituted pentamers could be obtained in high purity by flash chromatography on silica gel.

Thermal Properties. For the fabrication of vacuum-processed solar cells, the thermal stability of the applied donor materials is of crucial importance. Therefore, the thermal properties of the DCV-end-capped pentamers were investigated by thermogravimetric analysis (TGA) and differential scanning calorimetry (DSC) under an inert atmosphere at a heating rate of 10 °C/min (Figure 2). The excellent thermal stability of the oligomers was manifested in their TGA profile, showing decomposition temperatures (T_d) with 5% weight loss above 370 °C (Table 1). With an increase in selenophene units, T_d was found to be slightly decreased from 392 °C for **DCV5T** to 372 °C for co-oligomer **3**. Nevertheless, this indicates excellent thermal stability suitable for successful vacuum sublimation. In the DSC curves, one sharp endothermic peak indicating the melting temperature (T_m) is observed for each compound. With increasing number of selenophene units, the melting point gradually increases from 203 °C for **DCV5T** to 215 °C for co-oligomer **3**. All compounds start to decompose above 360−370 °C, which is indicated by a broad exothermic peak in the DSC curves.

Scheme 2. Synthesis of Compound 2[a]

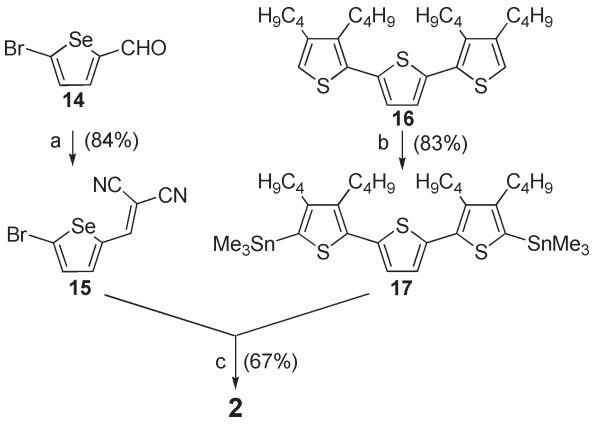

[a] (a) Malononitrile, β-alanine, DCE/EtOH, reflux, 17 h. (b) TMEDA, *n*-BuLi, THF, −78 to 50 °C. (c) $Pd(PPh_3)_4$, DMF, 75 °C, 16 h.

Optical Spectroscopy. The optical properties of the DCV-end-capped pentamers were investigated by UV−vis and fluorescence spectroscopy in solution (measured in dichloromethane) and in thin films (prepared by vacuum sublimation). The data are summarized in Table 1. Representative spectra for co-oligomer **3** are shown in Figure 3. The spectra of the other pentamers are similar and are omitted for clarity reasons.

In solution, all compounds showed one major absorption maximum between 510 and 540 nm, which corresponds to the $\pi-\pi^*$ (HOMO→LUMO) transition of the conjugated π-system. It is bathochromically shifted compared to unsubstituted quinquethiophenes or quinqueselenophenes[43,44] due to lowering of the LUMO energy by the electron-withdrawing DCV end groups.

The absorption maximum is gradually red-shifted with increasing number of selenophene units from 513 nm for **DCV5T** (without selenophenes) to 533 nm for **3** (three selenophenes). The pronounced red shift upon going from co-oligomer **1** to **2** seems to be due to the DCV-terminated selenophenes introduced at the periphery of the molecules. The selenophene in the middle of the molecule only leads to a small red shift as shown by comparison of compounds that differ only in the core selenophene, that is, **DCV5T** and **1** (shift from 513 to 516 nm) or **2** and **3** (shift from 529 to 533 nm). The molar extinction coefficient linearly increases with the number of selenophenes (62 600 $L \cdot mol^{-1} \cdot cm^{-1}$ for **DCV5T** to 66 000 $L \cdot mol^{-1} \cdot cm^{-1}$ for **3**). This correlation is illustrated in Figure 4.

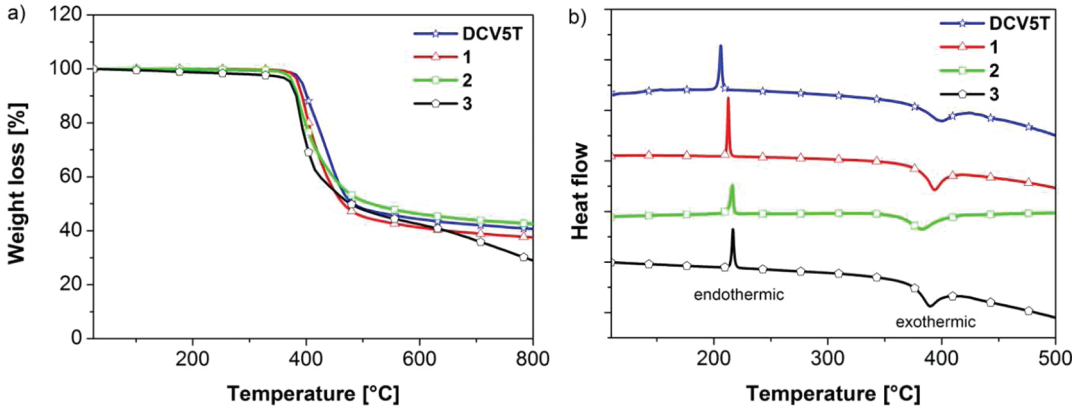

Figure 2. (a) TGA thermograms of DCV-end-capped pentamers **1**−**3** and **DCV5T** measured under N_2. Conditions: N_2 flow 50 mL/min, heating rate 10 °C/min. (b) DSC curves for mixed selenophene−thiophene oligomers **1**−**3** in comparison to **DCV5T** measured under argon flow at a heating rate of 10 °C/min.

dx.doi.org/10.1021/cm201392c |*Chem. Mater.* 2011, 23, 4435–4444

Table 1. Optical Data for Selenophene−Thiophene Pentamers

			solution				thin film		
compd	T_d[a]	T_m[b]	λ_{abs}(nm)	ε_{max} (L·mol^{-1}·cm^{-1})	λ_{em}(nm)	E_g^{opt} (eV)[c]	λ_{abs}(nm)	λ_{em}(nm)	E_g^{opt} (eV)[d]
DCV5T	392	203	513	62 600	661	2.02	573	726	1.76
1	384	211	516	63 600	667	2.01	577	735	1.74
2	375	213	529	64 900	675	1.96	589	737	1.72
3	372	215	533	66 000	673	1.93	592	758	1.67

[a] Decomposition temperature corresponding to 5% weight loss in N_2 determined by TGA. [b] Melting temperature determined from DSC. [c] Estimated from the onset of UV−vis spectra in DCM. [d] Estimated from the onset of UV−vis spectra of films prepared by vacuum sublimation.

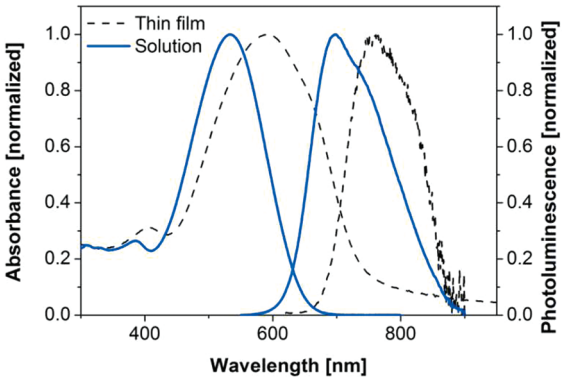

Figure 3. Representative UV−vis absorption and fluorescence spectra of pentamer **3**. Solution spectra were measured in dichloromethane. Thin films (30 nm) were prepared by vacuum sublimation.

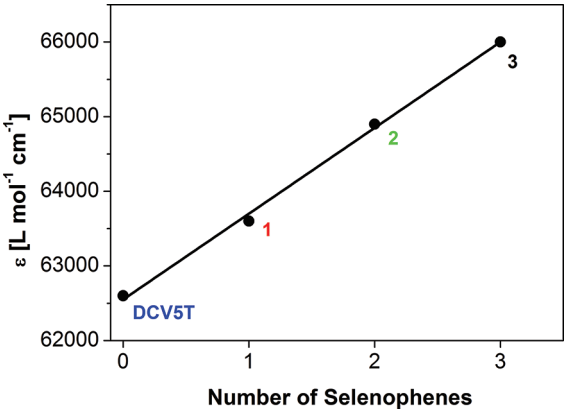

Figure 4. Correlation of molar extinction coefficients with number of selenophenes.

The fluorescence spectra of the pentamers are structureless and show a single emission maximum. An increasing number of selenophenes also leads to a red shift of the emission maximum from 661 nm for **DCV5T** to 675 nm for **2** in solution.

Thin film absorption and emission spectra are red-shifted by about 60−80 nm and significantly broadened compared to the corresponding solution spectra. This red shift is mainly caused by planarization and ordering of the molecules in the solid state, resulting in greater interchromophoric interactions and better packing in thin film. The optical band gaps (E_g^{opt}), which are calculated from onset of thin film absorption spectra, were 1.76−1.67 eV and about 0.25 eV lower than the values calculated

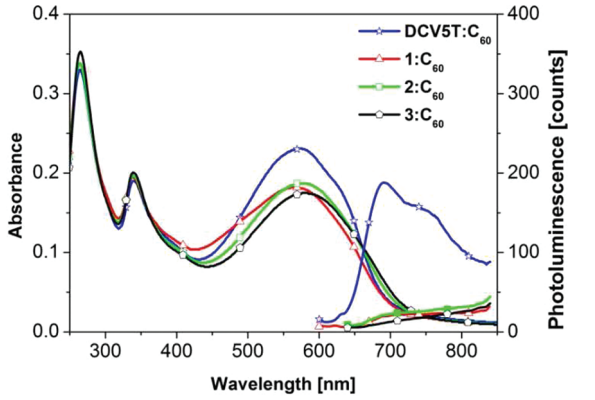

Figure 5. UV−vis absorption and fluorescence spectra of optimized donor−acceptor layers as used in bulk-heterojunction solar cells. Blend layers of all four compounds are shown, each with C_{60} in a mixing ratio of 2:1 (v/v) deposited on a heated substrate (90 °C).

from solution spectra. Also here, the gradual lowering of the band gap correlates with increasing number of selenophene units in the mixed oligomers.

In Figure 5, the absorption and emission spectra of the donor−acceptor blend layers are shown as they are used in the optimized bulk-heterojunction solar cells presented later in this paper. All four compounds were codeposited with C_{60} (2:1 by volume) on heated substrate (90 °C). All absorption spectra show an additional absorption peak at 340 nm and an increased absorption at around 450 nm compared to the pristine films, due to the C_{60} absorption. All four compounds show an absorption maximum at around 570 nm. In contrast to the absorption in solution, the blend layer with **DCV5T** shows the highest absorbance in this wavelength range. The absorbance of the co-oligomers is decreased by a factor of about 20%. The emission of the blend layer with **DCV5T** is reduced by about 2 orders of magnitude compared to the pristine **DCV5T** layer. Nevertheless, the photoluminescence is not completely quenched when the blend layer is deposited on heated substrate, which is a hint for phase separation of donor and acceptor leading to optimized charge carrier transport in the blend layer. In general, a fraction of the excitons generated in the larger domains of **DCV5T** are not able to reach the C_{60} interface, thus leading to inefficient quenching of the **DCV5T** luminescence.[18] In contrast, the luminescence of the blend layers with co-oligomers **1**−**3** is almost completely quenched by C_{60}. This behavior points toward a lower degree of donor−acceptor phase separation in the blend layer compared to **DCV5T**.

dx.doi.org/10.1021/cm201392c |*Chem. Mater.* 2011, 23, 4435–4444

Cyclic Voltammetry. Redox properties were determined by cyclic voltammetry in dichloromethane with $TBAPF_6$ (tetrabutylammonium hexafluorophosphate) as supporting electrolyte (0.1 M). The cyclovoltammograms are shown in Figure 6 and the data are summarized in Table 2. Additionally, the redox properties of thin films prepared by drop-casting from dichloromethane solution onto a platinum electrode were determined by cyclic voltammetry in acetonitrile with $TBAPF_6$ as supporting electrolyte (0.1 M) (see Figure S1 in Supporting Information). No significant change in the redox properties was observed with increasing number of selenophene units in the oligomers. All compounds showed two reversible oxidation waves at around 0.60 and 0.85 V, respectively, which indicate the formation of stable radical cations and dications as expected for pentamers. In the negative-potential regime, an irreversible reduction wave between −1.36 and −1.50 V was observed, which is assigned to the reduction of the DCV end groups. The oxidation potentials of co-oligomers **1** and **3** containing core selenophene units are somewhat lower than those of their thiophene counterparts **DCV5T** and **2**, reflecting the lower electronegativity of selenium.

HOMO and LUMO energy levels of all compounds were calculated from the onset of first oxidation and reduction waves, respectively, and data are presented in Table 2. In solution, the HOMO energies of all pentamers lie with slight variations between −5.61 and −5.57 eV, and the LUMO energy levels slightly vary from −3.74 to −3.80 eV. The HOMO energies in thin films lie between −5.63 and −5.68 eV, and the LUMO energies are in the range of −3.75 to −3.90 eV. The energy levels in solution and in thin films are in good agreement. All oligomers have relatively low-lying HOMO energy levels as a result of incorporation of the DCV acceptor end groups, which are beneficial for achieving a high V_{OC} in solar cells. These values are very similar to **DCV5T**, which lacks the selenophene moieties, and should be well suited for incorporation into SMOSCs.

The electrochemical band gaps (E_g^{CV}) obtained with these co-oligomers in solution are gradually decreased with increasing number of selenophene units (1.87 eV for **DCV5T** to 1.77 eV for co-oligomer **3**). In thin films, the band gaps lie in the same range, but the observed trend is not so clearly visible. The electrochemical band gaps are in good agreement with the optical band gaps (E_g^{opt}) determined from solution or thin-film spectra.

Solar Cell Characterizations. The DCV-end-capped thiophene−selenophene pentamers and **DCV5T** were used as electron-donor materials in coevaporated bulk-heterojunction solar cells with fullerene C_{60} as electron acceptor. The cells were prepared by vacuum sublimation following the m-i-p construction principle reported in the literature.[46]

The general device structure of the investigated solar cells is shown in Figure 7. An indium tin oxide (ITO) -coated glass substrate was first covered with a layer of C_{60} (15 nm), and then a donor−acceptor bulk-heterojunction layer (20 nm) was deposited by coevaporation of the respective mixed pentamer (donor) and C_{60} (acceptor). All devices were heated to a substrate temperature of approximately 90 °C during the deposition of the mixed layer. We expected a stronger phase separation when

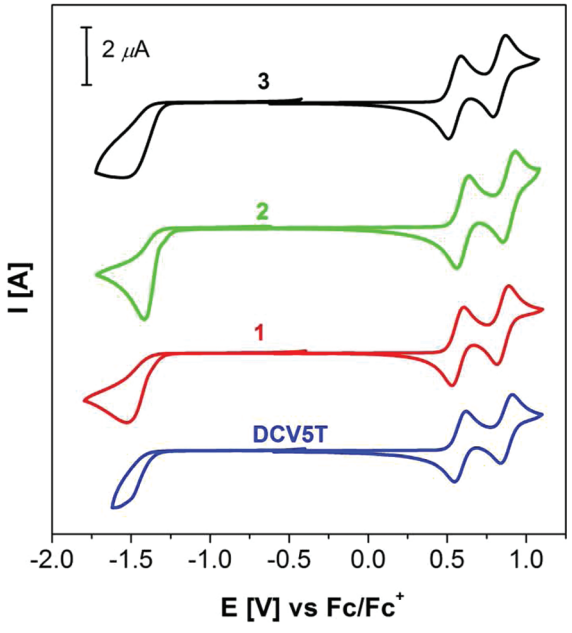

Figure 6. Cyclic voltammograms of mixed selenophene−thiophene oligomers, measured in DCM/$TBAPF_6$ (0.1 M), $c \approx 1 \times 10^{-3}$ mol·L^{-1}, 295 K, scan rate = 100 mV·s^{-1}.

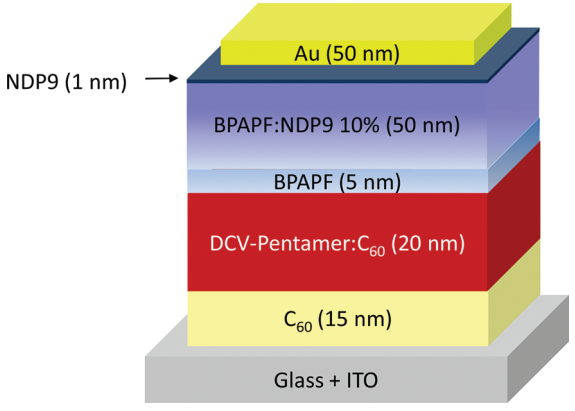

Figure 7. General device architecture of investigated BHJ solar cells.

Table 2. Electrochemical Data for Selenophene−Thiophene Pentamers and DCV5T[a]

				solution		thin film			
compd	E_{ox1} (V)	E_{ox2} (V)	E_{red1} (V)	HOMO[b] (eV)	LUMO[b] (eV)	HOMO[c] (eV)	LUMO[c] (eV)	E_g^{CV} soln[d]	E_g^{CV} film[d]
DCV5T	0.58	0.87	−1.50	−5.61	−3.74	−5.67	−3.75	1.87	1.92
1	0.57	0.86	−1.48	−5.60	−3.75	−5.68	−3.90	1.85	1.78
2	0.60	0.89	−1.36	−5.63	−3.80	−5.64	−3.89	1.83	1.75
3	0.55	0.83	−1.45	−5.58	−3.80	−5.63	−3.85	1.77	1.78

[a] Measured in DCM-$TBAPF_6$ (0.1 M), [compound] = 10^{-3} mol·L^{-1}, 25 °C, V = 100 mV·s^{-1}, vs Fc^+/Fc. [b] Measured in dichloromethane solution. [c] Drop-cast films on platin electrode measured in acetonitrile solution; set Fc^+/Fc; E_{HOMO} = −5.1 eV (ref 45). [d] Calculated from the difference between $E_{onset,\ red1}$ and $E_{onset,\ ox1}$.

dx.doi.org/10.1021/cm201392c |*Chem. Mater.* 2011, 23, 4435–4444

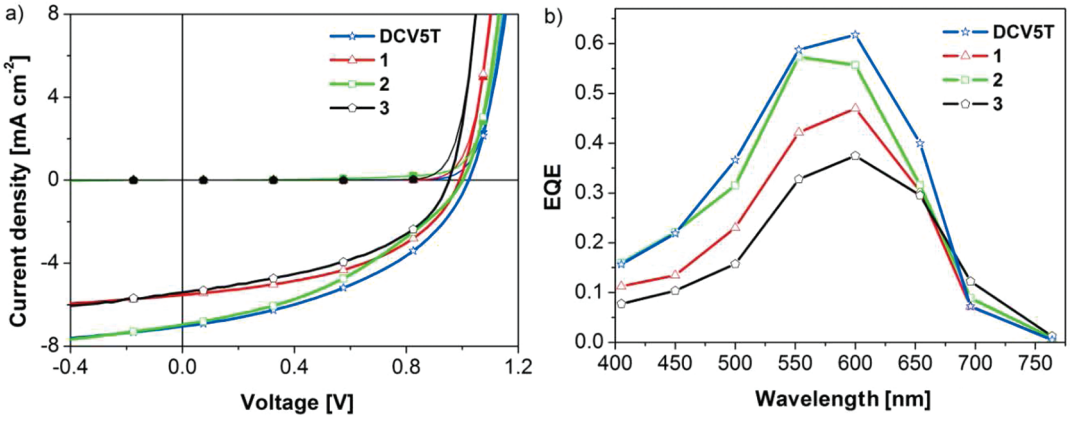

Figure 8. (a) $J-V$ characteristics of bulk-heterojunction solar cells with DCV-end-capped pentamers as donor materials. (b) Corresponding external quantum efficiency spectra of BHJ solar cells.

Table 3. Photovoltaic Parameters of Bulk-Heterojunction Solar Cells Containing DCV-End-Capped Selenophene−Thiophene Pentamers and DCV5T

compd	J_{SC} (mA·cm^{-2})	V_{OC} (V)	FF (%)	saturation[a]	incident light intensity (mW·cm^{-2})	$J_{SC,ap,100}$[b] (mA·cm^{-2})	η (%)
DCV5T	7.0	1.02	43	1.17	99	7.9	3.47
1	5.5	0.99	48	1.14	92	6.5	3.09
2	7.0	1.0	39	1.26	101	7.5	2.93
3	5.4	0.95	46	1.23	105	5.8	2.53

[a] Defined as $J(-1\ V)/J_{SC}$. [b] Measured with mask.

the substrate is heated during the deposition, providing better charge transport within the percolation pathways of the mixed layer.[18,20] This layer was covered with 5 nm of undoped and 50 nm of doped 9,9-bis[4-(*N*,*N*-bis-biphenyl-4-ylamino)phenyl]-9*H*-fluorene (BPAPF) as hole transport layer. The undoped BPAPF layer was introduced to avoid direct contact between the active layer and the doped BPAPF layer, which otherwise could lead to quenching of excitons by the dopants.[18] The thickness of the doped BPAPF layer was chosen to have the active layer approximately in the interference maximum. NDP9 (10 wt %) was used as p-dopant, and another layer of NDP9 (1 nm) was used between the hole transport layer (HTL) and the top Au electrode to facilitate charge extraction. The dopant material NDP9 was purchased from Novaled AG, Dresden, Germany. It can be used for doping of organic materials with low-lying HOMO energy levels and was chosen due to better stability and processability. The blend ratio of donor to acceptor is 2:1 by volume, which was found to be optimal for previously reported DCV derivatives.[12,20]

Figure 8a shows the $J-V$ characteristics of BHJ solar cells. The active area of the solar cells was approximately 6 mm^2. The photovoltaic parameters of these BHJ devices are summarized in Table 3. Since the correct active area of especially small organic solar cells is difficult to determine, the $J-V$ characteristics of each solar cell were measured with an aperture mask of 2.76 mm^2 as well. From this measurement, $J_{SC,ap,100}$ (normalized to 100 mW·cm^{-2}) and the power conversion efficiency (η) were calculated. The mismatch between the spectrum of the sun simulator and AM1.5G was not taken into account.

All devices measured under dark showed good rectification behavior. The open-circuit voltages (V_{OC}) obtained with all devices under illumination are in the range 0.95−1.02 V. The obtained high V_{OC} can be ascribed to the large energy difference between the HOMO of the donor and the LUMO of the C_{60} acceptor.

The short-circuit densities ($J_{SC,ap,100}$) showed values in the range 7.9−5.8 mA·cm^{-2}. The values match with the EQE spectra shown in Figure 8b within experimental error. The BHJ devices showed broad external quantum efficiency (EQE) covering from 400 to 750 nm, which are in good agreement with the thin-film absorption spectra. The difference in J_{SC} values seen in the $J-V$ curve is further reflected in the EQE spectra, with the **DCV5T** device showing the best EQE value of about 60% at around 600 nm. The increased J_{SC} value for **DCV5T** is further corroborated with the thin-film spectra of the donor/C_{60} blend layers, where **DCV5T** displayed higher absorbance compared to the selenophene-containing derivatives. Both compounds (**1** and **3**) with a selenophene substitution in the center of the molecule showed a significant decrease in $J_{SC,ap,100}$. This effect has already been observed by comparing absorption in solution and the absorption of the blend layers. One possible explanation is a lower degree of phase separation compared to **DCV5T**, leading to a lower degree of crystallinity in the DCV pentamer phase and thus to an increased intramolecular disorder, resulting in a decrease of absorption in the blended film.

In Table 3, the saturation of the photocurrent with reverse bias is also given. The saturation is defined by the current density under illumination at −1 V bias divided by J_{SC}. The devices showed saturation values between 1.14 and 1.26, which indicates that there is some recombination at short-circuit condition and in reverse bias. A saturation value close to unity corresponds to efficient charge separation and extraction, while a larger value hints at recombination losses and field-dependent dissociation of

dx.doi.org/10.1021/cm201392c |*Chem. Mater.* 2011, 23, 4435–4444

charge carriers. Devices with compounds **2** and **3** with selenophenes placed in direct contact with the DCV end group showed a significant increase in saturation. This voltage-dependent recombination of photogenerated charge carriers might be attributed either to a degradation in charge carrier transport in the blend layer or to a decrease in the probability of exciton separation at the donor−acceptor interface.

The efficiency decreased from 3.5% to 2.5% with increasing number of selenophenes. In the case of pentamers **1** and **3**, the decrease in η is caused by the lower J_{SC}, while in the case of **2**, the decrease in η is primarily caused by the lower fill factor (FF). Recently, McCulloch and Durrant and co-workers[35,47] reported a broad EQE spectrum for regioregular poly(3-hexylselenophene)/$PC_{61}BM$ device relative to the regioregular poly(3-hexylthiophene)/$PC_{61}BM$ device, while the peak EQE is significantly lower for the former. The result was ascribed to the relatively lower internal photocurrent generation efficiencies and poor charge transport of the former at the donor−acceptor interface.

CONCLUSION

In conclusion, we have prepared a series of novel A-D-A quinquechalcogenophenes for small-molecule organic solar cells. The co-oligomers/pentamers differ by the number and position of selenophene units in the π-conjugated backbone. Structures and purity were fully characterized by NMR, mass, and elemental analysis. The pentamers were further compared with oligothiophene **DCV5T**, which lacks the selenophene unit. All of the new co-oligomers exhibit excellent thermal stability. The increase in the number of selenophene units resulted in a bathochromic shift in the absorption spectra, thus lowering the optical band gap. A slight variation in the HOMO/LUMO energy levels determined from cyclic voltammetry resulted in a lowering of the band gap from 1.87 eV for **DCV5T** to 1.77 eV for co-oligomer **3**. Organic BHJ solar cells were fabricated by vacuum processing with these co-oligomers as electron donor and C_{60} as the electron acceptor. Under standard AM1.5G conditions, the highest PCE, ∼3.5%, was obtained for **DCV5T**. Despite broader and more intense absorption, Se-containing co-oligomers unexpectedly showed slightly lower performance compared to **DCV5T** in SMOSCs but still in a good range of 2.5−3.1%. The PCEs gradually decrease with increasing selenophene units. Photoluminescence study of blend layers pointed toward a lower degree of donor−acceptor phase separation for **1**-**3** in comparison to **DCV5T**. This study has shown the influence of molecular design on the device performance. The lowering of the optical band gap and HOMO/LUMO energies of A-D-A-type oligomers by varying the substitution pattern in the π-conjugated backbone is not the only criterion to obtain a good solar cell. There is still room for further optimization by carefully considering the charge-transport properties, charge separation, and dissociation at the donor−acceptor interface, and significant advances are anticipated in the near future for the design of this class of p-type semiconductors.

EXPERIMENTAL SECTION

Physical Measurements and Instrumentation. NMR spectra were recorded on a Bruker AMX 500 (^{1}H NMR, 500 MHz; ^{13}C NMR, 125 MHz) or an Avance 400 spectrometer (^{1}H NMR, 400 MHz; ^{13}C NMR, 100 MHz) at 25 °C unless otherwise noted. Chemical shift values (δ) are expressed in parts per million with residual solvent protons (^{1}H NMR, δ_H = 7.26 for $CDCl_3$; ^{13}C NMR, δ_C = 77.0 for $CDCl_3$) as internal standard. The splitting patterns are designated as follows: s (singlet), d (doublet), t (triplet), q (quartet), and m (multiplet). The assignments are Se−H (selenophene protons), Th−H (thiophene protons), −CHO (aldehyde protons), DCV-H (dicyanovinylene protons), Bu (butyl protons). Melting points were determined on a Mettler Toledo DSC 823^e and were not corrected. Elemental analyses were performed on an Elementar Vario EL. Thin-layer chromatography was carried out on aluminum plates, precoated with silica gel, Merck Si60 F_{254}. Preparative column chromatography was performed on glass columns packed with silica gel, Merck Silica 60, particle size 40−43 μm. EI mass spectra were recorded on a Varian Saturn 2000 GC-MS and MALDI-TOF mass spectra on a Bruker Daltonics Reflex III.

Optical measurements in solution were carried out in 1 cm cuvettes with Merck Uvasol-grade solvents. Absorption spectra were recorded on a Perkin-Elmer Lambda 19 spectrometer, and corrected fluorescence spectra were recorded on a Perkin-Elmer LS 55 fluorescence spectrometer. Cyclic voltammetry experiments were performed with a computer-controlled Autolab PGSTAT30 potentiostat in a three-electrode single-compartment cell with a platinum working electrode, a platinum wire counterelectrode, and an Ag/AgCl reference electrode. All potentials were internally referenced to the ferrocene/ferrocenium couple.

Thin Film and Device Fabrication. Thin films and heterojunction solar-cell devices were prepared by thermal vapor deposition in ultrahigh vacuum at a base pressure of 10^{-7} mbar onto the substrate at room temperature. Thin films for absorption and emission measurements were prepared on quartz substrates, solar cells on tin-doped indium oxide (ITO) coated glass (Thin Film Devices; sheet resistance of 30 $\Omega \cdot \text{square}^{-1}$). Layer thicknesses were determined during evaporation by using quartz crystal monitors calibrated for the respective material. The thin films prepared for absorption and emission measurements are approximately 30 nm thick. Thin film absorption spectra were recorded on a Shimadzu UV-2101/3101 UV−vis spectrometer. The thin film emission spectra were recorded with an Edinburgh Instruments FSP920 fluoresence spectrometer. Bulk-heterojunction solar cells were prepared layer by layer without breaking the vacuum. The layer structure of the bulk-heterojunction solar cells is as follows: ITO/15 nm C_{60}/20 nm blend layer of respective pentamer and C_{60} (ratio 2:1 in volume) prepared by coevaporation deposited on heated substrate (90 °C)/5 nm BPAPF/50 nm BPAPF doped with 10 wt % NDP9 (Novaled AG, Dresden, Germany)/1 nm NDP9/50 nm gold. The dopant material NDP9 was purchased from Novaled AG, Dresden, Germany, and is available by directly contacting the company.

Photovoltaic Characterization. $J-V$ and EQE measurements were carried out in a glovebox with nitrogen atmosphere. $J-V$ characteristics were measured on a source-measure unit (Keithley SMU 2400) and an AM 1.5G sun simulator (KHS Technical Lighting SC1200). The intensity was monitored with a silicon photodiode (Hamamatsu S1337), which was calibrated at Fraunhofer ISE. The mismatch between the spectrum of the sun simulator and the AM 1.5G spectrum was not taken into account. For well-defined active solar-cell areas, aperture masks (2.76 mm^2) were used. Simple EQE measurements were carried out by use of the sun simulator in combination with color filters for monochromatic illumination. The illumination intensities were measured with a silicon reference diode (Hamamatsu S1337).

Materials. Tetrahydrofuran (THF, Merck) was dried under reflux over sodium/benzophenone (Merck). Dimethylformamide (DMF, Merck) was dried under reflux over phosphorus pentoxide (Merck). Dichloromethane (DCM), $CHCl_3$, *n*-hexane, and diethyl ether were purchased from Merck and distilled prior to use. All synthetic steps were carried out under an argon atmosphere (except Knoevenagel condensations). Selenophene was purchased from Molekula, $HP(^tBu)_3BF_4$ from Alfa Aesar, and potassium carbonate from ABCR. *n*-Butyllithium (1.6 N in *n*-hexane) and $Pd_2(dba)_3 \cdot CHCl_3$ were purchased from Acros. *N*-Bromosuccinimide (NBS), iodine, mercury(II) acetate, phosphoryl

dx.doi.org/10.1021/cm201392c |*Chem. Mater.* 2011, 23, 4435–4444

chloride, and β-alanine were purchased from Merck. Malononitrile, trimethyltin chloride, 2-isopropoxy-4,4,5,5-tetramethyl[1,3,2]dioxaborolane (ITDB), and 2-(tributylstannyl)thiophene **10** were purchased from Aldrich.

5-Bromoselenophene-2-carbaldehyde[41] and 3,4,3″,4″-tetrabutyl-2,2′:5′,2″-terthiophene[42] were synthesized according to literature procedures.

Syntheses. *2,5-Dibromoselenophene (**5**).* In the absence of light, selenophene **4** (4.02 g, 30.7 mmol) was dissolved in dry DMF (25 mL) and the solution was degassed. NBS (10.88 g, 61.2 mmol) was added in four portions within 30 min, and afterward the orange solution was stirred at room temperature (rt) for 18 h. The reaction mixture was poured into ice−water (100 mL) and extracted with DCM (3 × 100 mL). The combined organic phases were washed with brine (100 mL) and water (2 × 100 mL) and dried over Na_2SO_4. Removal of the solvent yielded 10.1 g of an orange liquid, which was purified by column chromatography (silica; *n*-hexane). The pure product (7.46 g, 25.8 mmol, 84%) was obtained as a colorless liquid. ^{1}H NMR (400 MHz, $CDCl_3$) δ = 7.00 (s, 2H, H-3,4). ^{13}C NMR (100 MHz, $CDCl_3$) δ = 132.98 (C-3,4), 115.60 (C-2,5). MS (CI) m/z = 290 [M + H$^+$] (calcd for $C_4H_2Br_2Se$, 288.83).

*2,5-Bis(3,4-dibutylthien-2-yl)selenophene (**8**).* In a Schlenk tube and under argon, 2,5-dibromoselenophene **5** (3.99 g, 13.8 mmol) and 2-(3,4-dibutylthien-2-yl)-4,4,5,5-tetramethyl-1,3,2-dioxaborolane **7** (10.4 g, 32.3 mmol) were dissolved in degassed THF (40 mL). $Pd_2(dba)_3$ (243 mg, 266 μmol, 2 mol %) and HP^{t}Bu$_3$BF$_4$ (154 mg, 545 μmol, 4 mol %) were added, the solution was degassed again and 20 mL (40.0 mmol) of an aqueous K_3PO_4 solution (2 M) was added. The solution was stirred at 50 °C for 22 h. THF was mostly evaporated, 50 mL of water was added, and the mixture was extracted with DCM (3 × 50 mL). The combined organic layers were dried over Na_2SO_4 and the solvent was removed in vacuo. The crude product was purified by column chromatography (flash silica, *n*-hexane) to obtain the pure product **8** (5.86 g, 11.3 mmol, 82%) as an off-white solid, mp 56 °C. ^{1}H NMR (400 MHz, $CDCl_3$) δ = 7.21 (s with Se satellites, $^3J_{Se-H}$ = 5.2 Hz, 2H, Se−H), 6.85 (s, 2H, Th−H), 2.71 (t, ^3J = 7.8 Hz, 4H, α-Bu), 2.54 (t, ^3J = 7.8 Hz, 4H, α-Bu), 1.69 − 1.62 (m, 4H, β-Bu), 1.58 − 1.50 (m, 4H, β-Bu), 1.49−1.40 (m, 8H, γ-Bu), 0.98 (t, ^3J = 7.4 Hz, 6H, δ-Bu), 0.96 (t, ^3J = 7.4 Hz, 6H, δ-Bu). ^{13}C NMR (100 MHz, $CDCl_3$) δ = 143.61, 141.70, 138.50, 133.26, 127.81, 118.94, 32.76, 31.84, 28.93, 27.64, 23.01, 22.69, 14.02, 13.92. Anal. Calcd for $C_{28}H_{40}S_2Se$: C, 65.71; H, 7.76; S, 12.34. Found: C, 65.91; H, 7.69; S, 12.22.

*2,5-Bis(3,4-dibutyl-5-iodothien-2-yl)selenophene (**9**).* 2,5-Bis(3,4-dibutylthien-2-yl)selenophene **8** (2.89 g, 5.56 mmol) was dissolved in dry chloroform (100 mL) and the solution was degassed. At 0 °C, mercury(II) acetate (3.72 g, 11.7 mmol) was added, and the solution was stirred at 0 °C for 15 min and then overnight at rt. The orange solution was cooled back to 0 °C and iodine (2.96 g, 11.7 mmol) was added. The solution became greenish blue; it was stirred at 0 °C for 30 min and then at rt for 4 h. The resulting solid was filtered off and washed thoroughly with chloroform, and the filtrate was washed with sodium disulfite solution (100 mL). The aqueous phase was extracted with chloroform and DCM. The combined organic layers were dried over Na_2SO_4 and the solvent was removed in vacuum. The crude product was purified by column chromatography (flash silica, *n*-hexane). The pure product **9** (4.06 g, 5.26 mmol, 95%) was obtained as a yellow solid, mp 96 °C. ^{1}H NMR (400 MHz, $CDCl_3$) δ = 7.15 (s, 2H, Se−H), 2.73 (virtual t, 4H, α-Bu), 2.53 (virtual t, 4H, α-Bu), 1.55−1.39 (m, 16H, β-Bu + γ-Bu), 0.98 (t, ^3J = 7.0 Hz, 6H, δ-Bu), 0.94 (t, ^3J = 7.2 Hz, 6H, δ-Bu). ^{13}C NMR (100 MHz, $CDCl_3$) δ = 147.59, 140.91, 138.39, 138.13, 128.22, 74.29, 33.05, 32.08, 31.05, 28.40, 22.93, 22.86, 13.93, 13.86. MS (MALDI-TOF) m/z [M$^+$] = 772.0 (calcd for $C_{28}H_{38}I_2S_2Se$, 771.97). Anal. calcd for $C_{28}H_{38}I_2S_2Se$: C, 43.59; H, 4.96; S, 8.31. Found: C, 43.44; H, 4.88; S, 8.44.

*4,4,5,5-Tetramethyl-2-(selenophen-2-yl)-1,3,2-dioxaborolane (**11**).* Selenophene **4** (3.04 g, 23.2 mmol) was dissolved under argon in dry THF (30 mL) and the solution was cooled to −78 °C. At this temperature, *n*-butyllithium (1.6 M in hexane, 14.8 mL, 23.7 mmol) was added dropwise during 20 min. The yellow solution was stirred at −78 °C for 1 h. ITDB (4.47 g, 24.1 mmol) was added dropwise during 20 min and the turbid mixture was allowed to slowly warm to rt. It became yellow and clear and was stirred at rt for 16 h. The solvent was removed in vacuum (not to dryness) and a saturated NH_4Cl solution (30 mL) was added. It was extracted with DCM (3 × 30 mL), and the combined organic layers were washed with brine (50 mL) and water (50 mL) and dried over Na_2SO_4. Removal of the solvent afforded the crude product as an orange oil, which quickly crystallized. The resulting yellowish crystals were dried under high vacuum and 5.60 g (21.8 mmol, 94%) of pure product was obtained. ^{1}H NMR (400 MHz, $CDCl_3$) δ = 8.37 (dd with Se satellites, ^3J = 5.2 Hz, ^4J = 0.8 Hz, $^2J_{H-Se}$ = 45.2 Hz, 1H, Se−H-5), 7.95 (dd with Se satellites, ^3J = 3.6 Hz, ^4J = 0.8 Hz, $^2J_{H-Se}$ = 13.6 Hz, 1H, Se−H-3), 7.46 (dd, ^3J = 5.2 Hz, ^3J = 3.6 Hz, 1H, Se−H-4), 1.35 (s, 12H, −CH_3). ^{13}C NMR (100 MHz, $CDCl_3$) δ = 139.56, 137.63, 130.96, 84.09, 24.77. MS (CI) m/z = 258 [M + H$^+$] (calcd for $C_{10}H_{15}BO_2Se$, 257.00). Anal. Calcd for $C_{10}H_{15}BO_2Se$: C, 46.73; H, 5.88. Found: C, 46.66; H, 5.83.

*2,5-Bis(3,4-dibutyl-2,2′-bithien-5-yl)selenophene (**12a**).* In a Schlenk tube and under argon, 2,5-bis(3,4-dibutyl-5-iodothien-2-yl)selenophene **9** (1.41 g, 1.84 mmol) and 2-(tributylstannyl)thiophene **10** (2.76 g, 7.18 mmol) were dissolved in dry degassed THF (20 mL). $Pd(PPh_3)_2Cl_2$ (51.5 mg, 73.5 μmol, 4 mol %) and cesium fluoride (550 mg, 3.62 mmol) were added, and the solution was degassed and stirred at 75 °C for 90 h. THF was evaporated, water (50 mL) was added, and the mixture was extracted with DCM (3 × 50 mL). The combined organic phases were washed with water (50 mL) and dried over Na_2SO_4 and the solvent was removed. The crude product was purified by column chromatography (flash silica, hexane/DCM 9:1). The pure product (1.18 g, 1.73 mmol, 94%) was obtained as an orange solid, mp 102 °C. ^{1}H NMR (400 MHz, $CDCl_3$) δ = 7.32 (d, ^3J = 5.2 Hz, 2H, Th−H), 7.25 (s, 2H, Se−H), 7.15 (d, ^4J = 2.8 Hz, 2H, Th−H), 7.07 (dd, ^3J = 5.2 Hz, ^4J = 3.6 Hz, 2H, Th−H), 2.75−2.68 (m, 8H, α-Bu), 1.63−1.39 (m, 16H, β-Bu + γ-Bu), 0.98 (t, ^3J = 7.2 Hz, 6H, δ-Bu), 0.96 (t, ^3J = 7.6 Hz, 6H, δ-Bu). ^{13}C NMR (100 MHz, $CDCl_3$) δ = 140.93, 140.20, 139.74, 136.10, 132.10, 129.84, 127.90, 127.36, 125.83, 125.31, 33.01, 32.90, 28.11, 27.84, 23.10, 23.00, 13.90, 13.87. MS (MALDI-TOF) m/z [M$^+$] = 684.2 (calcd for $C_{36}H_{44}S_4Se$, 684.15). Anal. Calcd for $C_{36}H_{44}S_4Se$: C, 63.22; H, 6.48; S, 18.75. Found: C, 63.34; H, 6.37; S, 18.63.

*2,5-Bis[3,4-dibutyl-5-(selenophen-2-yl)thien-2-yl]selenophene (**12b**).* 2,5-Bis(3,4-dibutyl-5-iodothien-2-yl)selenophene **9** (1.47 g, 1.90 mmol) and 4,4,5,5-tetramethyl-2-(selenophen-2-yl)-1,3,2-dioxaborolane **11** (1.23 g, 4.79 mmol) were dissolved in dry THF (22 mL) and the solution was degassed. $Pd_2(dba)_3 \cdot CHCl_3$ (39 mg, 37.7 μmol, 2 mol %) and HP^{t}Bu$_3$BF$_4$ (21.8 mg, 75.1 μmol, 4 mol %) were added, the solution was degassed again and 5.8 mL (11.6 mmol) of a degassed 2 M aqueous K_3PO_4 solution were added. The reaction mixture was stirred at rt overnight. THF was mostly distilled off, the residue was redissolved in DCM, and water (50 mL) was added. The organic layers were separated and the aqueous layer was extracted with DCM (2 × 50 mL). The combined organic layers were dried over Na_2SO_4 and the solvent was removed. The crude product was purified by column chromatography (flash silica, hexane/DCM 9:1) to obtain product **12b** (1.42 g, 1.82 mmol, 96%) as an orange solid, mp 110 °C. ^{1}H NMR (400 MHz, $CDCl_3$) δ = 8.00 (dd with Se satellites, ^3J = 4.4 Hz, ^4J = 2.4 Hz, $^2J_{H-Se}$ = 47.0 Hz, 2H, Se−H), 7.32−7.28 (m, 4H, Se−H), 7.25 (s with Se satellites, $^3J_{H-Se}$ = 5.2 Hz, 2H, Se−H), 2.75−2.67 (m, 8H, α-Bu), 1.62−1.41 (m, 16H, β-Bu + γ-Bu), 0.97 (t, ^3J = 7.2 Hz, 6H, δ-Bu), 0.96 (t, ^3J = 7.2 Hz, 6H, δ-Bu). ^{13}C NMR (100 MHz, $CDCl_3$) δ = 141.01, 140.87, 139.89, 139.83, 132.23, 132.11, 130.95, 129.82, 127.96, 127.90, 33.00, 32.92, 28.16, 27.91, 23.10, 23.02, 13.90, 13.87. MS (MALDI-TOF) m/z [M$^+$] = 778.1 (calcd for $C_{36}H_{44}S_2Se_3$, 778.04). Anal. Calcd for $C_{36}H_{44}S_2Se_3$: C, 55.59; H, 5.70; S, 8.25. Found: C, 55.79; H, 5.52; S, 8.29.

*5′,5″-(Selenophene-2,5-diyl)bis(3′,4′-dibutyl-2,2′-bithiophene-5-carbaldehyde) (**13a**).* DMF (1.29 g, 17.6 mmol) and phosphoryl chloride (2.70 g, 17.6 mmol) were dissolved under argon in 12 mL of dichloroethane, and the solution was stirred at rt for 2 h. 2,5-Bis(3,4-dibutyl-2,2′-bithien-5-yl)selenophene **12a** (600 mg, 0.88 mmol) was dissolved under argon in dichloroethane (15 mL) and the Vilsmeier reagent was added. The solution turned from yellow to deep red. It was stirred at rt for 21 h. Saturated $NaHCO_3$ solution (50 mL) was added, and the mixture was stirred for 1.5 h at rt. It was extracted with DCM (3 × 50 mL), the combined organic layers were washed with water (50 mL) and dried over Na_2SO_4, and the solvent was removed. The crude product was purified by column chromatography (flash silica, traces of monoaldehyde eluted with DCM, dialdehyde eluted with DCM/EtOAc 95:5). The pure product (578 mg, 0.78 mmol, 89%) was obtained as a red solid, mp 96 °C. ^{1}H NMR (400 MHz, $CDCl_3$) δ = 9.89 (s, 2H, −CHO), 7.71 (d, ^3J = 4.0 Hz, 2H, Th−H), 7.30 (s, 2H, Se−H), 7.25 (d, ^3J = 4.0 Hz, 2H, Th−H), 2.80−2.71 (m, 8H, α-Bu), 1.62−1.43 (m, 16H, β-Bu + γ-Bu), 0.98 (t, ^3J = 7.2 Hz, 12H, δ-Bu). ^{13}C NMR (100 MHz, $CDCl_3$) δ = 182.61, 146.19, 142.68, 142.14, 140.93, 140.54, 136.87, 134.23, 128.94, 128.61, 126.90, 32.92, 32.53, 28.14, 28.04, 23.05, 23.01, 13.86. MS (MALDI-TOF) m/z [M^+] = 739.5 (calcd for $C_{38}H_{44}O_2S_4Se$, 740.14). Anal. Calcd for $C_{38}H_{44}O_2S_4Se$: C, 61.68; H, 5.99; S, 17.33. Found: C, 61.79; H, 5.98; S, 17.51.

*5,5′-[5,5′-(Selenophene-2,5-diyl)bis(3,4-dibutylthien-5,2-diyl)]diselenophene-2-carbaldehyde (**13b**).* DMF (945 mg, 12.9 mmol) and phosphoryl chloride (1.99 g, 13.0 mmol) were dissolved under argon in 10 mL of dichloroethane, and the solution was stirred at rt for 2 h. 2,5-Bis[3,4-dibutyl-5-(selenophen-2-yl)thien-2-yl]selenophene **12b** (502 mg, 0.65 mmol) was dissolved under argon in 15 mL of dichloroethane and the Vilsmeier reagent was added. The solution turned from yellow to deep red. It was stirred at rt for 22 h. Saturated $NaHCO_3$ solution (50 mL) was added and the mixture was stirred for 2 h at rt. It was extracted with DCM (3 × 50 mL), the combined organic layers were washed with water (50 mL) and dried over Na_2SO_4, and the solvent was removed. The crude product was purified by column chromatography (flash silica, traces of monoaldehyde eluted with DCM, dialdehyde eluted with DCM/EtOAc 95:5). The pure product **13b** (507 mg, 0.61 mmol, 94%) was obtained as a red solid, mp 107 °C. ^{1}H NMR (400 MHz, $CDCl_3$) δ = 9.78 (s with Se satellites, $^3J_{H-Se}$ = 4.4 Hz, 2H, −CHO), 7.94 (d, ^3J = 4.2 Hz, 2H, Se−H), 7.43 (d, ^3J = 4.2 Hz, 2H, Se−H), 7.31 (s, 2H, Se−H), 2.78−2.71 (m, α-Bu), 1.63−1.43 (m, 16H, β-Bu + γ-Bu), 0.98 (t, ^3J = 7.0 Hz, 12H, δ-Bu). ^{13}C NMR (100 MHz, $CDCl_3$) δ = 183.98, 151.11, 148.21, 142.50, 140.90, 140.65, 139.83, 134.22, 131.66, 128.62, 128.03, 32.93, 32.57, 28.31, 28.10, 23.08, 23.06, 13.87, 13.86. MS (MALDI-TOF) m/z [M^+] = 834.5 (calcd for $C_{38}H_{44}O_2S_2Se_3$, 834.03). Anal. Calcd for $C_{38}H_{44}O_2S_2Se_3$: C, 54.74; H, 5.32; S, 7.69. Found: C, 54.81; H, 5.32; S, 7.78.

*2,2′-[5′,5″-(Selenophene-2,5-diyl)bis(3′,4′-dibutyl-2,2′-bithien-5′,5-diyl)]bis(methan-1-yl-1-ylidene)dimalononitrile (**1**).* 5′,5″-(Selenophene-2,5-diyl)bis(3′,4′-dibutyl-2,2′-bithiophene-5-carbaldehyde) **13a** (275 mg, 0.372 mmol), malononitrile (73.4 mg, 1.11 mmol), and β-alanine (4.00 mg, 44.9 μmol) were dissolved in a dichloroethane/ethanol mixture (25 mL, 1:1 v/v), and the solution was refluxed for 24 h. The solvent was evaporated and the residue was purified by column chromatography (flash silica, DCM). The pure product **1** (279 mg, 0.334 mmol, 90%) was obtained as a green solid with a metallic gleam, mp 211 °C. ^{1}H NMR (400 MHz, $CDCl_3$) δ = 7.77 (s, 2H, DCV−H), 7.69 (d, ^3J = 4.4 Hz, 2H, Th−H), 7.34 (s, 2H, Se−H), 7.29 (d, ^3J = 4.4 Hz, 2H, Th−H), 2.84−2.79 (m, 4H, α-Bu), 2.77−2.72 (m, 4H, α-Bu), 1.63−1.44 (m, 16H, β-Bu + γ-Bu), 1.00 (t, ^3J = 7.2 Hz, 6H, δ-Bu), 0.99 (t, ^3J = 6.8 Hz, 6H, δ-Bu). ^{13}C NMR (100 MHz, $CDCl_3$) δ = 149.89, 148.35, 144.11, 139.17, 133.96, 129.00, 128.60, 126.14, 75.80, 32.87, 32.41, 28.05, 23.04, 23.01, 13.86. MS (MALDI-TOF) m/z [M^+] = 836.5 (calcd for $C_{44}H_{44}N_4S_4Se$, 836.16). Anal. Calcd for $C_{44}H_{44}N_4S_4Se$: C, 63.21; H, 5.30; N, 6.70. Found: C, 63.15; H, 5.15; N, 6.78.

*2,2′-{5,5′-[5,5′-(Selenophene-2,5-diyl)bis(3,4-dibutylthien-5,2-diyl)]bis(selenophene-5,2-diyl)}bis(methan-1-yl-1-ylidene)dimalononitrile (**3**).* 5,5′-[5,5′-(Selenophene-2,5-diyl)bis(3,4-dibutylthien-5,2-diyl)]-diselenophene-2-carbaldehyde **13b** (236 mg, 0.283 mmol), malononitrile (58.2 mg, 0.881 mmol), and β-alanine (2.20 mg, 24.7 μmol) were dissolved in a dichloroethane/ethanol mixture (20 mL, 1:1 v/v), and the solution was refluxed for 24 h. The solvent was evaporated and the residue was purified by column chromatography (flash silica, DCM). The pure product **3** (208 mg, 0.224 mmol, 79%) was obtained as a green solid with a metallic gleam, mp 215 °C. ^{1}H NMR (400 MHz, $CDCl_3$) 7.84 (s, 2H, DCV−H), 7.82 (d, ^3J = 4.4 Hz, 2H, Se−H), 7.43 (d, ^3J = 4.4 Hz, 2H, Se−H), 7.35 (s, 2H, Se−H), 2.81−2.73 (m, 8H, α-Bu), 1.63−1.44 (m, 16H, β-Bu + γ-Bu), 1.00 (t, ^3J = 7.2 Hz, 6H, δ-Bu), 0.99 (t, ^3J = 7.2 Hz, 6H, δ-Bu). ^{13}C NMR (100 MHz, $CDCl_3$) δ = 154.59, 152.97, 143.98, 143.40, 141.19, 140.99, 138.99, 135.72, 131.36, 129.03, 127.29, 114.39, 114.02, 75.50, 32.86, 32.33, 28.60, 28.11, 23.05, 13.87, 13.80. MS (MALDI-TOF) m/z [M^+] = 930.5 (calcd for $C_{44}H_{44}N_4S_2Se_3$, 930.05). Anal. Calcd for $C_{44}H_{44}N_4S_2Se_3$: C, 56.83; H, 4.77; N, 6.03. Found: C, 56.94; H, 4.77; N, 5.97.

*5,5″-Bis(trimethylstannyl)-3,4,3″,4″-tetrabutyl-2,2′:5′,2″-terthiophene (**17**).* 3,4,3″,4″-Tetrabutyl-2,2′:5′,2″-terthiophene **16** (2.00 g, 4.23 mmol) was dissolved under argon in absolute THF (12 mL) and absolute hexane (7 mL), and TMEDA was added. The solution was stirred at rt for 30 min. At −78 °C, *n*-BuLi (1.6 M in hexane, 6.25 mL, 10.0 mmol) was added dropwise within 30 min; the solution was warmed to rt and then stirred at 50 °C for 25 min. A solution of trimethyltin chloride (2.00 g, 10.0 mmol) in absolute THF (7 mL) was added at −78 °C, and the mixture was stirred at rt for 3 days. Saturated NH_4Cl solution (120 mL) was added and the mixture was extracted with diethyl ether (3 × 150 mL); the combined organic layers were dried over $MgSO_4$, and the solvent was removed. After drying in high vacuum, product **17** (2.82 g, 3.50 mmol, 83%) was obtained as an orange oil. ^{1}H NMR (400 MHz, $CDCl_3$) δ = 7.03 (s, 2H, Th−H), 2.73 (t, 4H, ^3J = 7.9 Hz, α-Bu), 2.55 (t, 4H, ^3J = 7.5 Hz, α-Bu), 1.58−1.38 (m, 16H, β-Bu + γ-Bu), 0.97 (t, 6H, ^3J = 7.2 Hz, δ-Bu), 0.97 (t, 6H, ^3J = 7.2 Hz, δ-Bu), 0.39 (s, 18H, Me). ^{13}C NMR (100 MHz, $CDCl_3$) δ = 151.29, 139.86, 136.79, 136.52, 125.45, 34.96, 33.02, 31.51, 27.73, 23.19, 23.11, 13.99, 13.89, 7.81. The product was used without further purification.

*2-[(5-Bromoselenophen-2-yl)methylene]malononitrile (**15**).* 5-Bromoselenophene-2-carbaldehyde **14** (2.15 g, 9.04 mmol), malononitrile (1.50 g, 22.7 mmol), and β-alanine (53.0 mg, 0.59 mmol) were dissolved in ethanol (30 mL). The solution was stirred at 60 °C for 15 h and then cooled to rt. The resulting solid was filtered off, washed with ethanol, and dried in high vacuum to obtain the pure product (2.16 mg, 7.56 mmol, 84%) as yellow crystals, mp 183 °C. ^{1}H NMR (400 MHz, $CDCl_3$) δ = 7.83 (d with Se satellites, ^4J = 0.6 Hz, $^3J_{Se-H}$ = 8.1 Hz, DCV−H), 7.59 (dd, ^3J = 4.3 Hz, ^4J = 0.6 Hz, Se−H-3), 7.43 (d, ^3J = 4.3 Hz, Se−H-4). ^{13}C NMR (100 MHz, $CDCl_3$) 153.23, 142.45, 141.94, 134.11, 131.93, 113.49, 113.39, 78.44. MS (CI) m/z = 286 [M^+] (calcd for $C_8H_3BrN_2Se$, 285.99). Anal. Calcd for $C_8H_3BrN_2Se$: C, 33.60; H, 1.06; N, 9.80. Found: C, 33.75; H, 1.13; N, 10.00.

*5,5″-Bis[5-(2,2-dicyanovinylene)selenophen-2,5-diyl]-3,4,3″,4″-tetrabutyl-[2,2′:5′,2″]terthiophene (**2**).* In a Schlenk tube, DCV-substituted bromoselenophene **15** (322 mg, 1.13 mmol) and distannylterthiophene **17** (300 mg, 0.376 mmol) were dissolved under argon in dry DMF (4 mL), and the mixture was degassed. $Pd(PPh_3)_4$ (4 mg, 3 μmol) was added, and the mixture was degassed again and then stirred at 75 °C for 3 days. Water (30 mL) was added and the mixture was extracted with DCM (30 mL). The organic layer was dried over Na_2SO_4, and the solvent was removed in vacuo. The crude product was purified by column chromatography (silica, DCM/*n*-hexane 4:1). The pure product **2** (223 mg, 0.253 mmol, 67%) was obtained as a green solid, mp 213 °C. ^{1}H NMR ($CDCl_3$, 400 MHz) δ = 7.84 (s with Se satellites, $^3J_{Se-H}$ = 9.0 Hz, 2H, DCV−H), 7.82 (d, ^3J = 4.5 Hz, 2H, Se−H), 7.43 (d, ^3J = 4.5 Hz,

dx.doi.org/10.1021/cm201392c |*Chem. Mater.* 2011, 23, 4435–4444

2H, Se−H), 7.19 (s, 2H, Th−H), 2.83−2.73 (m, 8H, α-Bu), 1.63−1.55 (m, 8H, β-Bu), 1.54−1.45 (m, 8H, γ-Bu), 1.00 (t, ^3J = 7.5 Hz, 6H, δ-Bu), 0.99 (t, ^3J = 7.5 Hz, 6H, δ-Bu). ^{13}C NMR ($CDCl_3$, 125 MHz, 320 K) δ = 154.61, 152.79, 143.82, 142.99, 141.60, 138.94, 136.17, 133.36, 131.51, 127.55, 127.10, 114.25, 113.92, 76.13, 32.79, 32.45, 28.59, 28.01, 23.04, 22.99, 13.78, 13.73. (MALDI-TOF) m/z [M^+] = 884.2 (calcd for $C_{44}H_{44}N_4S_3Se_2$, 884.1). Anal. Calcd for $C_{44}H_{44}N_4S_3Se_2$: C, 59.85; H, 5.02; N, 6.35. Found: C, 59.97; H, 5.14; N, 6.47.

■ ASSOCIATED CONTENT

Supporting Information. Ten figures, showing plots of cyclic voltammograms on thin films and ^{1}H NMR, ^{13}C NMR, and MALDI-TOF mass spectra of oligomers **1**−**3**. This material is available free of charge via the Internet at http://pubs.acs.org/.

■ AUTHOR INFORMATION

Corresponding Author

*E-mail amaresh.mishra@uni-ulm.de (A.M.) or peter.baeuerle@uni-ulm.de (P.B.).

■ ACKNOWLEDGMENT

We thank the German Ministry of Education and Research (BMBF) for financial support in the framework of Project OPEG 2010.

■ REFERENCES

(1) Brabec, C. J.; Sariciftci, N. S.; Hummelen, J. C. *Adv. Funct. Mater.* **2001**, *11*, 15–26.
(2) Günes, S.; Neugebauer, H.; Sariciftci, N. S. *Chem. Rev.* **2007**, *107*, 1324–1338.
(3) Walzer, K.; Maennig, B.; Pfeiffer, M.; Leo, K. *Chem. Rev.* **2007**, *107*, 1233–1271.
(4) Kippelen, B.; Brédas, J.-L. *Energy Environ. Sci.* **2009**, *2*, 251–261.
(5) Tang, C. W. *Appl. Phys. Lett.* **1986**, *48*, 183–185.
(6) Cheng, Y.-J.; Yang, S.-H.; Hsu, C.-S. *Chem. Rev.* **2009**, *109*, 5868–5923.
(7) Park, S. H.; Roy, A.; Beaupre, S.; Cho, S.; Coates, N.; Moon, J. S.; Moses, D.; Leclerc, M.; Lee, K.; Heeger, A. J. *Nat. Photonics* **2009**, *3*, 297–302.
(8) Chen, H.-Y.; Hou, J.; Zhang, S.; Liang, Y.; Yang, G.; Yang, Y.; Yu, L.; Wu, Y.; Li, G. *Nat. Photonics* **2009**, *3*, 649–653.
(9) Walker, B.; Kim, C.; Nguyen, T.-Q. *Chem. Mater.* **2010**, *23*, 470–482.
(10) Würthner, F.; Meerholz, K. *Chem.—Eur. J.* **2010**, *16*, 9366–9373.
(11) Boudreault, P.-L. T.; Najari, A.; Leclerc, M. *Chem. Mater.* **2011**, *23*, 456–469.
(12) Fitzner, R.; Reinold, E.; Mishra, A.; Mena-Osteritz, E.; Ziehlke, H.; Körner, C.; Leo, K.; Riede, M.; Weil, M.; Tsaryova, O.; Weiss, A.; Uhrich, C.; Pfeiffer, M.; Bäuerle, P. *Adv. Funct. Mater.* **2011**, *21*, 897–910.
(13) Wei, G.; Wang, S.; Sun, K.; Thompson, M. E.; Forrest, S. R. *Adv. Energy Mater.* **2011**, *1*, 184–187.
(14) Green, M. A.; Emery, K.; Hishikawa, Y.; Warta, W. *Prog. Photovoltaics* **2011**, *19*, 84–92.
(15) Schulze, K.; Uhrich, C.; Schüppel, R.; Leo, K.; Pfeiffer, M.; Brier, E.; Reinold, E.; Bäuerle, P. *Adv. Mater.* **2006**, *18*, 2872–2875.
(16) Uhrich, C.; Schueppel, R.; Petrich, A.; Pfeiffer, M.; Leo, K.; Brier, E.; Kilickiran, P.; Bäuerle, P. *Adv. Funct. Mater.* **2007**, *17*, 2991–2999.
(17) Schueppel, R.; Schmidt, K.; Uhrich, C.; Schulze, K.; Wynands, D.; Brédas, J. L.; Brier, E.; Reinold, E.; Bu, H. B.; Bäuerle, P.; Maennig, B.; Pfeiffer, M.; Leo, K. *Phys. Rev. B* **2008**, *77*, No. 085311.
(18) Wynands, D.; Levichkova, M.; Riede, M.; Pfeiffer, M.; Bäuerle, P.; Rentenberger, R.; Denner, P.; Leo, K. *J. Appl. Phys.* **2010**, *107*, No. 014517.
(19) Kronenberg, N. M.; Steinmann, V.; Bürckstümmer, H.; Hwang, J.; Hertel, D.; Würthner, F.; Meerholz, K. *Adv. Mater.* **2010**, *22*, 4193–4197.
(20) Wynands, D.; Levichkova, M.; Leo, K.; Uhrich, C.; Schwartz, G.; Hildebrandt, D.; Pfeiffer, M.; Riede, M. *Appl. Phys. Lett.* **2010**, *97*, 073503.
(21) Mishra, A.; Uhrich, C.; Reinold, E.; Pfeiffer, M.; Bäuerle, P. *Adv. Energy Mater.* **2011**, *1*, 265–273.
(22) Steinberger, S.; Mishra, A.; Reinold, E.; Levichkov, J.; Uhrich, C.; Pfeiffer, M.; Bäuerle, P. *Chem. Commun.* **2011**, *47*, 1982–1984.
(23) Steinberger, S.; Mishra, A.; Reinold, E.; Müller, C. M.; Uhrich, C.; Pfeiffer, M.; Bäuerle, P. *Org. Lett.* **2011**, *13*, 90–93.
(24) Brabec, C. J.; Cravino, A.; Meissner, D.; Sariciftci, N. S.; Fromherz, T.; Rispens, M. T.; Sanchez, L.; Hummelen, J. C. *Adv. Funct. Mater.* **2001**, *11*, 374–380.
(25) Scharber, M. C.; Mühlbacher, D.; Koppe, M.; Denk, P.; Waldauf, C.; Heeger, A. J.; Brabec, C. J. *Adv. Mater.* **2006**, *18*, 789–794.
(26) Schulze, K.; Riede, M.; Brier, E.; Reinold, E.; Bäuerle, P.; Leo, K. *J. Appl. Phys.* **2008**, *104*, No. 074511.
(27) Mishra, A.; Ma, C.-Q.; Bäuerle, P. *Chem. Rev.* **2009**, *109*, 1141–1276.
(28) Nakanishi, H.; Inoue, S.; Otsubo, T. *Mol. Cryst. Liq. Cryst.* **1997**, *296*, 335–348.
(29) Heeney, M.; Zhang, W.; Crouch, D. J.; Chabinyc, M. L.; Gordeyev, S.; Hamilton, R.; Higgins, S. J.; McCulloch, I.; Skabara, P. J.; Sparrowe, D.; Tierney, S. *Chem. Commun.* **2007**, 5061–5063.
(30) Patra, A.; Wijsboom, Y. H.; Zade, S. S.; Li, M.; Sheynin, Y.; Leitus, G.; Bendikov, M. *J. Am. Chem. Soc.* **2008**, *130*, 6734–6736.
(31) Zade, S. S.; Zamoshchik, N.; Bendikov, M. *Chem.—Eur. J.* **2009**, *15*, 8613–8624.
(32) Hollinger, J.; Jahnke, A. A.; Coombs, N.; Seferos, D. S. *J. Am. Chem. Soc.* **2010**, *132*, 8546–8547.
(33) Zade, S. S.; Zamoshchik, N.; Bendikov, M. *Acc. Chem. Res.* **2011**, *44*, 14–24.
(34) Yang, R.; Tian, R.; Yan, J.; Zhang, Y.; Yang, J.; Hou, Q.; Yang, W.; Zhang, C.; Cao, Y. *Macromolecules* **2004**, *38*, 244–253.
(35) Ballantyne, A. M.; Chen, L.; Nelson, J.; Bradley, D. D. C.; Astuti, Y.; Maurano, A.; Shuttle, C. G.; Durrant, J. R.; Heeney, M.; Duffy, W.; McCulloch, I. *Adv. Mater.* **2007**, *19*, 4544–4547.
(36) Chung, D. S.; Kong, H.; Yun, W. M.; Cha, H.; Shim, H.-K.; Kim, Y.-H.; Park, C. E. *Org. Electron.* **2010**, *11*, 899–904.
(37) Qiao, F. E. N.; Hou, X.; Lu, Y.; Chen, H.; Liu, A.; Hu, X.; Siu Choon, N. *Sol. Energy Mater. Sol. Cells* **2010**, *94*, 442–445.
(38) Gao, F.; Cheng, Y.; Yu, Q.; Liu, S.; Shi, D.; Li, Y.; Wang, P. *Inorg. Chem.* **2009**, *48*, 2664–2669.
(39) Li, R.; Lv, X.; Shi, D.; Zhou, D.; Cheng, Y.; Zhang, G.; Wang, P. *J. Phys. Chem. C* **2009**, *113*, 7469–7479.
(40) Mazzio, K. A.; Yuan, M.; Okamoto, K.; Luscombe, C. K. *ACS Appl. Mater. Interfaces* **2011**, *3*, 271–278.
(41) Antonov, D. N.; Belen'Kii, L. I.; Gronowitz, S. *J. Heterocycl. Chem.* **1995**, *32*, 53–55.
(42) Krömer, J.; Bäuerle, P. *Tetrahedron* **2001**, *57*, 3785–3794.
(43) Nakanishi, H.; Inoue, S.; Otsubo, T. *Mol. Cryst. Liq. Cryst.* **1997**, *296*, 335–348.
(44) Otsubo, T.; Takimiya, K. Selenophenes as hetero-analogues of thiophene-based materials. In *Handbook of Thiophene-Based Materials: Applications in Organic Electronics and Photonics*; Perepichka, I. F., Perepichka, D. F., Eds.; Wiley−VCH: Weinheim, Germany, 2009; pp 321−340.
(45) Johansson, T.; Mammo, W.; Svensson, M.; Andersson, M. R.; Inganäs, O. *J. Mater. Chem.* **2003**, *13*, 1316.
(46) Drechsel, J.; Männig, B.; Gebeyehu, D.; Pfeiffer, M.; Leo, K.; Hoppe, H. *Org. Electron.* **2004**, *5*, 175–186.
(47) Clarke, T. M.; Ballantyne, A. M.; Tierney, S.; Heeney, M.; Duffy, W.; McCulloch, I.; Nelson, J.; Durrant, J. R. *J. Phys. Chem. C* **2010**, *114*, 8068–8075.